Thermal Coupling Reactions of 1-Phenyl-3,4-dimethylphosphole within the Coordination Sphere of Palladium(II)

William L. Wilson,[†] Jean Fischer,[‡] Roderick E. Wasylishen,[§] Klaus Eichele,[§] Vincent J. Catalano,[†] John H. Frederick,[†] and John H. Nelson*,[†]

Department of Chemistry, University of Nevada, Reno, Nevada 89557, Department of Chemistry, Dalhousie University, Halifax, Nova Scotia, Canada B3H 4J3, and Laboratoire de Cristallochimie et de Chimie Structurale (URA 424-CNRS), Université Louis Pasteur, 67070 Strasbourg Cedex, France

Received October 12, 1995[⊗]

The thermolyses of dihalobis(1-phenyl-3,4-dimethylphosphole)palladium(II) complexes [$(DMPP)_2PdX_2$, X = Cl, Br, I] were investigated in 1,1,2,2-tetrachloroethane solutions at 145 °C and in the crystalline state at 140 °C. For *cis*-$(DMPP)_2$ $PdCl_2$ and *cis*- or *trans*-$(DMPP)_2$ $PdBr_2$ four types of products were formed: (1) [4 + 2] cycloaddition products, (2) [2 + 2] cycloaddition products, (3) compounds that result from 1,5-hydrogen migration from a methyl group on one phosphole to the β-carbon of an adjacent phosphole (*exo*-methylene), and (4) products that result from an intermolecular [4 + 2] coupling of two phospholes followed sequentially by phosphinidene elimination and intramolecular [4 + 2] cycloaddition to another phosphole to give diphosphatetracyclotetradecatrienes (DPTCT). *trans*-$(DMPP)_2PdBr_2$ undergoes thermal isomerization to *cis*-$(DMPP)_2PdBr_2$ in the solid state, and *cis*- and *trans*-$(DMPP)_2PdBr_2$ give the same products in both their solid- and solution-state thermolyses. In contrast, *trans*-$(DMPP)_2$ PdI_2 neither isomerizes to the *cis*-isomer nor undergoes any of the phosphole coupling reactions in either the solution or solid state. The crystal structures of *trans*-$(DMPP)_2PdX_2$ (X = Br, I), {-$(DMPP)_2$[2 + 2]}$PdBr_2$, {$(DMPP)_2$(*exo*-methylene)}$PdBr_2$, and (DPTCT)$PdCl_2$ were determined. They crystallize in the monoclinic $P2_1/c$, triclinic $P\bar{1}$, monoclinic $P2_1/c$, monoclinic $P2_1/n$, and orthorhombic $P2_12_12_1$ space groups in units cells of the following dimensions: $a = 10.158$ (3) Å, $b = 14.876$ (4) Å, $c = 16.829$ (5) Å, $\beta = 104.25(2)°$, $\rho_{calc} = 1.732$ g/cm^3, $Z = 4$; $a = 9.025(1)$ Å, $b = 11.023(1)$ Å, $c = 13.833$ (1) Å, $\alpha = 101.15(1)°$, $\beta = 98.82(1)°$, $\gamma = 105.30(1)°$, $\rho_{calc} = 1.886$ g/cm^3, $Z = 2$; $a = 13.090$ (2) Å, $b = 17.637$ (2) Å, $c = 21.834$ (2) Å, $\beta = 100.51$ (1)°, $\rho_{calc} = 1.738$ g/cm^3, $Z = 4$, $a = 10.721$ (1) Å, $b = 16.929$ (1) Å, $c = 14.675(1)$ Å, $\beta = 97.86$ (1)°, $\rho_{calc} = 1.663$ g/cm^3, $Z = 4$; and $a = 15.532$ (3) Å, $b = 19.401$ (4) Å, $c = 9.910$ (2) Å, $\rho_{calc} = 1.490$ g/cm^3, $Z = 2$, respectively. Least-squares refinements converged at final values of $R(F)$ of 0.041, 0.0354, 0.0624, 0.0533, and 0.035 for 2770, 2672, 2729, 2159, and 2525 independent observed reflections, respectively. Kinetic studies suggest that the reaction mechanisms are the same in both the solid and solution states and that the reaction mechanisms are substantially different from those previously reported for the thermolyses of the analogous *cis*-$(DMPP)_2PtX_2$ complexes.

Introduction

Thermal[1,2] and photochemical[3,4] dimerization of 1-substituted-3,4-dimethylphospholes occurs within the coordination spheres of various transition metals. In each case where a [4 + 2] cycloaddition product results, only the *exo*-diastereomer is formed and these cycloaddition reactions are intramolecular. In contrast, intermolecular cycloadditions of dienophiles to free phospholes[5] (reaction 1) or [4 + 2] cyclodimerizations of

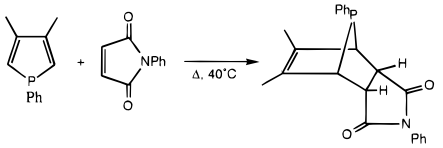

(1)[5]

phosphole oxides and phosphole sulfides (reaction 2) normally

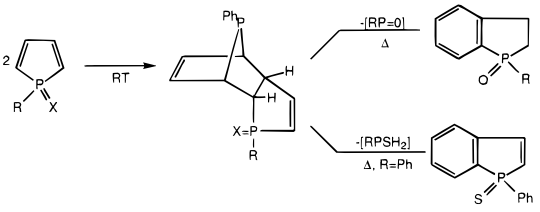

(2)

produce only the *endo*-diastereomers.[6−11] The latter are thermally unstable[12,13] and are converted to dihydrophosphindole oxides and phosphindole sulfides, respectively, upon thermolysis.

The differences in the products of thermolysis of $(DMPP)_2NiX_2$[1] and $(DMPP)_2PtX_2$[2] are striking, particularly since both reactions involve four coordinate complexes of metals from the same family. Within a given family, second and third row transition metals generally exhibit similar chemical reactions which are usually distinct from those of their first row congeners. The differences in the chemical behavior of the second and third row transition elements are mostly due to differences in their reaction rates which are usually 3−4 orders of magnitude faster

* Author to whom correspondence should be addressed.
† University of Nevada.
‡ Universite Louis Pasteur.
§ Dalhousie University.
⊗ Abstract published in *Advance ACS Abstracts,* February 15, 1996.

(1) Mercier, F.; Mathey, F.; Fischer, J.; Nelson, J. H. *J. Am. Chem. Soc.* **1984**, *106*, 425; *Inorg. Chem.* **1985**, *24*, 4141.
(2) Wilson, W. L.; Rahn, J. A.; Alcock, N. W.; Fischer, J.; Frederick, J. H.; Nelson, J. H. *Inorg. Chem.* **1994**, *33*, 109.
(3) Santini, C. C.; Fischer, J.; Mathey, F.; Mitschler, A. *J. Am. Chem. Soc.* **1980**, *102*, 5809.
(4) Ji, H.-L.; Nelson, J. H.; Fischer, J. *Phosphorus, Sulfur Silicon Relat. Elem.* **1993**, *77*, 268.
(5) Mathey, F.; Mercier, F. *Tetrahedron Lett.* **1981**, *22*, 319.

0020-1669/96/1335-1486$12.00/0

for the second row element. Marked differences in the reactions of analogous platinum and palladium complexes are not common.[14] Therefore, the thermolyses of dihalobis(1-phenyl-3,4-dimethylphosphole)palladium(II) complexes might be expected to mimic those of their platinum(II) counterparts.[2] As we show in this paper, there are differences in the intramolecular reactions and the palladium complexes exhibit a novel intermolecular reaction as well.[15]

Experimental Section

A. Reagents and Physical Measurements. All chemicals were reagent grade and were used as received or synthesized as described below. Solvents were dried by standard procedures and stored over Linde type 4 Å molecular sieves. All syntheses were conducted under a dry nitrogen atmosphere. The 1-phenyl-3, 4-dimethylphosphole was prepared by the literature method.[16] Elemental analyses were performed by Galbraith Laboratories, Knoxville, TN. Infrared spectra were recorded on a Perkin-Elmer 1800 FT-IR instrument as Nujol mulls on polyethylene thin films. Melting points were obtained using a Mel-Temp melting point apparatus and are uncorrected. All ^{31}P MAS NMR spectra were recorded on a Bruker MSL-200 spectrometer at 80.0 MHz. Cross-polarization from protons to ^{31}P under the Hartman−Hahn match condition and high-power decoupling were employed with typical ^{1}H 90° pulses of 4.0−10.0 μs and contact times of 3−5 ms. Spectra were referenced with respect to 85% H_3PO_4(aq) by setting the ^{31}P resonance of solid $NH_4H_2PO_4$ to 0.81 ppm. Solution ^{1}H, ^{1}H{^{31}P}, ^{13}C{^{1}H}, and ^{31}P{^{1}H} NMR spectra were recorded at 500, 500, 125, and 202.4 MHz, respectively, on a Varian unity plus 500 MHz NMR spectrometer. Proton and carbon chemical shifts are relative to internal Me_4Si, while phosphorus chemical shifts are relative to external 85% H_3PO_4(aq) with positive values being downfield of the respective reference.

B. Syntheses. *cis*-Dichlorobis(1-phenyl-3,4-dimethylphosphole)-palladium(II), *cis*-(DMPP)$_2$PdCl$_2$. To a vigorously stirred emulsion of 5.00 g (28.2 mmol) of $PdCl_2$ dissolved in 150 mL of 1 M aqueous sodium chloride and 150 mL of dichloromethane was added, under nitrogen via syringe, 10.5 mL (55.8 mmol) of 1-phenyl-3,4-dimethylphosphole. The aqueous phase became paler, and the organic phase became yellow. The reaction mixture was stirred overnight, whereupon the aqueous phase became pale pink and the organic phase deep yellow. The organic phase was removed by separatory funnel, dried with anhydrous magnesium sulfate, and gravity filtered into a 500 mL round-bottom flask. The solvent was removed by rotary evaporation using a water bath. The temperature of the water bath was gradually raised from room temperature to boiling over a period of about 1 h. The removal of the dichloromethane in this manner resulted in a foamy glass. The flask was removed hot from the rotary evaporator, and just enough benzene was added to the hot flask to dissolve the foamy glass. The flask was allowed to cool undisturbed, whereupon 1−5 mm crystals of the title compound slowly grew from the solution. These were isolated by gravity filtration, rinsed with diethyl ether, and allowed to air-dry (yield 12.85 g, 83.2%). Another crop of crystals could be obtained by removing the solvent from the mother liquor, redissolving in dichloromethane, and repeating the process (overall yield: 14.78 g, 95.7%). The compound isolated in this manner is identical to that prepared previously[17] but with no impurities derived from dimerization of the ligand in the recrystallization process or trace quantities of excess phosphole. Anal. Calcd for $C_{24}H_{26}Cl_2P_2Pd$: C, 52.08; H, 4.70; Cl, 12.81. Found: C, 51.89; H, 4.65; Cl, 12.68.

***trans*-Dibromobis(1-phenyl-3,4-dimethylphosphole)palladium-(II), *trans*-(DMPP)$_2$PdBr$_2$.** The preparation of this complex is similar to that of *cis*-(DMPP)$_2$PdCl$_2$. To a vigorously stirred emulsion of 5.00 g (28.2 mmol) of $PdCl_2$ dissolved in 150 mL of saturated aqueous potassium bromide solution and 150 mL of dichloromethane was added, under nitrogen via syringe, 10.5 mL (55.8 mmol) of 1-phenyl-3,4-dimethylphosphole. Isolation, as above, afforded 15.03 g (83.9%) of bright orange crystals of *trans*-dibromobis(1-phenyl-3,4-dimethylphosphole)palladium(II), mp 234−236 °C. IR (Nujol cm^{-1}) υ_{PdP}, 375, υ_{PdBr}, 200 cm^{-1}. Anal. Calcd for $C_{24}H_{26}Br_2P_2Pd$: C, 44.87; H, 4.05; Br, 24.88. Found: C, 44.58; H, 4.00; Br, 24.76.

***cis*-Dibromobis(1-phenyl-3,4-dimethylphosphole)palladium(II), *cis*-(DMPP)$_2$ PdBr$_2$.** A dilute solution of *trans*-dibromobis(1-phenyl-3,4-dimethylphosphole)palladium(II) in an acetone−water mixture was prepared by dissolving the complex in acetone and then slowly adding water until the mixture became cloudy. Then acetone was added to give a clear solution. The flask was covered with a tissue and set in a place far from the *trans* complex. As the acetone slowly evaporated, small bright yellow needles of *cis*-dibromobis(1-phenyl-3,4-dimethylphosphole)palladium(II) crystallized from the solution. These were collected by gravity filtration and allowed to air-dry, mp 229−231 °C (dec.). IR (Nujol cm^{-1}) υ_{PdP}, 395, 376; υ_{PdBr} 203, 180. Anal. Calcd for $C_{24}H_{26}Br_2P_2Pd$: C, 44.87; H, 4.05; Br, 24.88. Found: C, 44.69; H, 4.02; Br, 24.72.

***trans*-Diiodobis(1-phenyl-3,4-dimethyphosphole)palladium(II), *trans*-(DMPP)$_2$PdI$_2$.** The preparation of this compound is similar to that of *cis*-(DMPP)$_2$PdCl$_2$. To a vigorously stirred emulsion of 1.00 g (5.64 mmol) $PdCl_2$ dissovled in 30 mL of saturated aqueous sodium iodide solution and 30 mL of dichloromethane was added, under nitrogen via syringe, 2.1 mL (11.2 mmol) of 1-phenyl-3,4-dimethylphosphole. Isolation as for *cis*-(DMPP)$_2$PdCl$_2$ afforded 3.76 g (91.5%) of deep red crystals of *trans*-diiodobis(1-phenyl-3,4-dimethylphosphole)palladium(II), mp 234−237 °C (dec.). ^{31}P{^{1}H} NMR ($CDCl_3$): δ 9.51. ^{1}H NMR ($CDCl_3$): δ 2.11(s, 12H, CH_3), 7.06 (T, $|^2J(PH) + {}^4J(PH)| = 29.86$ Hz, 4H, H_α), 7.23−7.8 (m, 10H, Ph). ^{13}C-{^{1}H} NMR ($CDCl_3$): δ 17.6 (T, $|^3J(PC) + {}^5J(PC)| = 12.7$ Hz, CH_3), 127.8 (T, $|^1J(PC) + {}^3J(PC)| = 48.0$ Hz, C_i), 128.4 (T, $|^3J(PC) + {}^5J(PC)| = 10.7$ Hz, C_m), 130.2 (T, $|^1J(PC) + {}^3J(PC)| = 53.7$ Hz, C_α), 130.5 (s, C_p), 133.4 (T, $|^2J(PC) + {}^4J(PC)| = 13.7$ Hz, C_o), 152.5 (T, $|^2J(PC) + {}^4J(PC)| = 14.6$ Hz, C_β). Anal. Calcd for $C_{24}H_{26}I_2P_2Pd$: C, 39.14; H, 3.53. Found: C, 39.26; H, 3.45.

Solution Preparation of (DPTCT)PdCl$_2$. *cis*-Dichlorobis(1-phenyl-3, 4-dimethylphosphole)palladium(II), 1.00 g, was dissolved in 125 mL of 1,1,2,2-tetrachloroethane in a 250 mL round-bottom flask fitted with a reflux condenser and an N_2 outlet. The solution was heated at reflux for 30 h. A ^{31}P{^{1}H} NMR spectrum of the reaction mixture showed that the relative amounts of (DPTCT)PdCl$_2$, the [2 + 2], and *exo*-methylene products were 2.6:1:1.2. The reaction mixture was filtered, and the solution was allowed to sit uncovered in air at ambient temperature until all of the tetrachloroethane had evaporated, leaving bright yellow crystals in a red tar. The tar was dissolved in dichloroethane, leaving 0.20 g of (DPTCT)PdCl$_2$

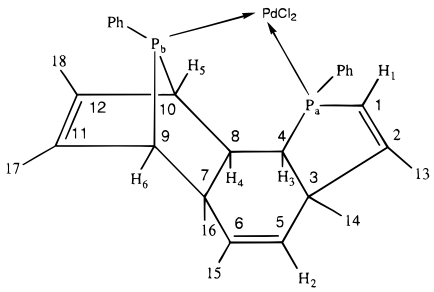

as bright yellow crystals which were recrystallized from methanol/water to yield 0.18 g, mp 263−266 °C (dec.). ^{31}P{^{1}H} NMR ($CDCl_3$): δ 34.84 (d, $^2J(PP) = 28.10$ Hz, P_a), 97.60 (d, $^2J(PP) = 28.10$ Hz, P_b). ^{1}H NMR ($CDCl_3$): δ 1.27 (d, $^4J(P_bH) = 1.20$ Hz, 3H, CH_3(17)), 1.35 (apparent t, $^4J(P_bH) = {}^4J(H_5CH_3) = 1.20$ Hz, 3H, CH_3(18)), 1.42 (d, $^4J(P_aH) = 1.20$ Hz, 3H, CH_3(14)), 1.59 (s, 3H, CH_3(16)), 2.07 (dd,

(6) Mathey, F.; Mankowski-Favelier, R. *Org. Magn. Reson.* **1972**, *4*, 171.
(7) Mathey, F., Lampin, J. P.; Thavard, D. *Can. J. Chem.* **1976**, *54*, 2402.
(8) Markl, G.; Potthast, R. *Tetrahedron Lett.* **1968**, 1755.
(9) Mathey, F. *Tetrahedron* **1972**, *28*, 4171.
(10) Usher, D. A.; Westheimer, F. H. *J. Am. Chem. Soc.* **1964**, *86*, 4732.
(11) Quin, L. D.; Szewczyk, J. *J. Chem. Soc., Chem. Commun.* **1986**, 844.
(12) Hughes, A. N.; Phisithkul, S.; Rukachaisirikul, T. *J. Heterocycl. Chem.* **1979**, *16*, 1417.
(13) Holah, D. G.; Hughes, A. N.; Kleemola, D. *J. Heterocycl. Chem.* **1977**, *14*, 705.
(14) Hartley, F. R. *The Chemistry of Platinum and Palladium;* Wiley: New York, 1973.
(15) An abstract of some of this work has been published; Wilson, W. L.; Nelson, J. H.; Rahn, J. A.; Alcock, N. W.; Fischer, J. *Phosphorus, Sulfur Silicon Relat. Elem.* **1993**, *77*, 29.
(16) Breque, A.; Mathey, F.; Savignac, P. *Synthesis* **1981**, 983.
(17) MacDougall, J. J.; Nelson, J. H.; Mathey, F.; Mayerle, J. J. *Inorg. Chem.* **1980**, *19*, 709.

$^4J(P_aH) = 2.10$ Hz, $^4J(H_1H) = 1.20$ Hz, 3H, $CH_3(13)$), 2.28 (d, $^4J(H_2$-$CH_3) = 1.50$ Hz, 3H, $CH_3(15)$), 2.33 (apparent dt, $^3J(P_bH) = 1.50$ Hz, $^4J(H_5H_6) = {}^3J(H_4H_5) = 0.90$ Hz, 1H, H_5), 2.55 (dddd, $^3J(P_aH) = 24.94$ Hz, $^3J(P_bH) = 21.94$ Hz, $^3J(H_3H_4) = 8.41$ Hz, $^3J(H_4H_5) = 0.9$ Hz, 1H, H_4), 3.11 (ddd, $^2J(P_aH_3) = 13.22$ Hz, $^3J(H_3H_4) = 8.41$ Hz, $^4J(P_bH_3) = 3.0$ Hz, 1H, H_3), 3.66 (dd, $^3J(P_bH_6) = 1.50$ Hz, $^4J(H_5H_6) = 0.90$ Hz, 1H, H_6), 5.39 (q, $^4J(H_2CH_3(15)) = 1.50$ Hz, 1H, H_2), 6.19 (dq, $^2J(PaH_1) = 27.05$ Hz, $^4J(H_1CH_3(13)) = 1.20$ Hz, 1H, H_1), 7.2−8.1 (m, 10H, Ph). CH_3OH and H_2O were detected in the ^1H NMR spectrum in approximately the correct ratios. $^{13}C\{^1H\}$ NMR ($CDCl_3$): δ 14.55 (s, $CH_3(18)$), 16,66 (d, $^3J(P_bC) = 3.02$ Hz, $CH_3(16)$), 17.49 (d, $^3J(P_aC) = 13.32$ Hz, $CH_3(13)$), 20.75 (s, $CH_3(15)$), 22.09 (d, $^3J(P_aC) = 6.66$ Hz, $CH_3(14)$), 30.50 (d, $^3J(P_bC) = 8.55$ Hz, $CH_3(17)$), 42.88 (d, $^2J(P_bC) = 18.86$ Hz, C_8), 47.07 (d, $^2J(P_bC) = 20.49$ Hz, C_7), 49.01 (dd, $^1J(P_bC) = 33.31$ Hz, $^3J(P_aC) = 21.37$ Hz, C_{10}), 50.38 (d, $^2J(P_aC) = 11.19$ Hz, C_3), 54.37 (dd, $^1J(P_aC) = 37.31$ Hz, $^3J(P_bC) = 3.48$ Hz, C_4), 57.09 (dd, $^1J(P_bC) = 33.27$ Hz, $^3J(P_aC) = 3.86$ Hz, C_9), 117.28 (d, $^1J(P_aC) = 59.71$ Hz, C_1), 124.16 (s, C_5), 127.97 (d, $^1J(PC) = 54.81$ Hz, C_i), 128.15 (d, $^3J(PC) = 10.69$ Hz, C_m), 129.28 (d, $^3J(PC) = 11.69$ Hz, C_m), 129.74 (d, $^3J(PC) = 48.27$ Hz, C_i), 130.70 (s, C_p), 132.07 (d, $^2J(PC) = 8.05$ Hz, C_o), 132.72 (s, C_p), 134.62 (d, $^2J(PC) = 13.07$ Hz, C_o), 135.58 (d, $^2J(P_bC) = 23.13$ Hz, C_{11} or C_{12}), 141.56 (s, C_6), 163.94 (d, $^2J(P_bC) = 8.17$ Hz, C_{12} or C_{11}). Anal. Calcd for $C_{30}H_{34}Cl_2P_2Pd\cdot 0.5\ CH_3OH\cdot H_2O$: C, 54.87; H, 5.69; Cl, 10.62. Found: C, 54.67; H, 5.42; Cl, 10.39.

Solid-State Preparation of (DPTCT)$PdCl_2$, Thermolysis of Dichlorobis(1-phenyl-3,4-dimethylphosphole)palladium(II). *cis*-$(DMPP)_2PdCl_2$ (1.00 g) was sealed in a break-seal ampule under nitrogen and heated in an oven at 140 °C for 30 h. The solid was dissolved in 1,1,2,2-tetrachloroethane, and the solution was filtered. The relative amounts of (DPTCT)$PdCl_2$, the [2 + 2], and *exo*-methylene products were determined by $^{31}P\{^1H\}$ NMR spectroscopy to be 2.4:1:1.4. Isolation as above afforded 0.16 g of the title complex as bright yellow crystals.

Solution Preparation of [$(DMPP)_2$(*exo*-methylene)]$PdBr_2$.

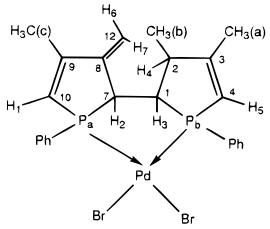

trans-$(DMPP)_2PdBr_2$ (1.00 g) was dissolved in 125 mL of 1,1,2,2-tetrachloroethane in a 250 mL round-bottom flask fitted with a reflux condenser and an N_2 outlet. The solution was brought to reflux and heated at reflux for 18 h. A $^{31}P\{^1H\}$ NMR spectrum of the reaction mixture showed that the relative amounts of (DPTCT)$PdBr_2$, the [2 + 2] and *exo*-methylene products were 1:1:2. The reaction mixutre was filtered, and the solution was allowed to sit at ambient temperature until the tetrachloroethane had evaporated, leaving orange-brown crystals in a brown tar. The tar was dissolved in 1,2-dichloroethane, leaving 0.39 g of crystalline *exo*-methylene compound as orange-brown crystals, mp 278−280 °C (dec.). $^{31}P\{^1H\}$ NMR ($CDCl_3$): δ 108.47 (d, $^2J(PP) = 16.97$ Hz, P_a), 94.62 (d, $^2J(PP) = 16.97$ Hz, P_b). ^1H NMR ($CDCl_3$): δ 1.29 (d, $^3J(H_4CH_3) = 6.91$ Hz, 3H, $CH_3(b)$), 1.94 (apparent dt, $^4J(P_bCH_3) = 2.4$ Hz, $^4J(H_5CH_3) = {}^4J(H_4H_3) = 1.2$ Hz, 3H, $CH_3(a)$), 2.32 (apparent t, $^4J(P_aCH_3) = {}^4J(H_1CH_3) = 1.5$ Hz, 3H, $CH_3(c)$), 2.34 (dqq, $^3J(H_3H_4) = 7.81$ Hz, $^3J(H_4, CH_3(b)) = 6.91$ Hz, $^4J(H_4, CH_3(a)) = 1.2$ Hz, 1H, H_4) 2.87 (dddd, $^3J(P_aH_3) = 43.28$ Hz, $^2J(P_bH_3) = 10.82$ Hz, $^3J(H_2H_3) = 9.95$ Hz, $^3J(H_3H_4) = 7.81$ Hz, 1H, H_3), 3.47 (dd, $_2J(H_2H_3) = 9.95$ Hz, $^2J(P_aH_2) = 5.11$ Hz, 1H, H_2), 5.38 (s, 1H, H_6 or H_7) , 5.76 (s, 1H, H_7 or H_6), 6.33 (dq, $^2J(P_bH_5) = 27.95$ Hz, $^4J(H_5$-$CH_3(a)) = 1.2$ Hz, 1H, H_5), 6.76 (dq, $^2J(P_aH_1) = 28.55$ Hz, $^4J(H_1, CH_3$-$(c)) = 1.5$ Hz, 1H, H_1), 7.35−7.92 (m, 10H, Ph). H_2O was detected in the ^1H NMR spectrum in approximately the correct ratio. $^{13}C\{^1H\}$ NMR ($CDCl_3$): δ 16.92 (d, $^3J(P_aC) = 13.00$ Hz, $CH_3(c)$), 19.63 (d, $^3J(P_bC) = 15.95$ Hz, $CH_3(a)$), 22.50 (dd, $^3J(P_bC) = 5.78$ Hz, $^4J(P_aC) = 2.16$ Hz, $CH_3(b)$), 46.15 (d, $^2J(P_bC) = 9.75$ Hz, C_2), 50.00 (dd, $^1J(P_aC) = 37.30$ Hz, $^2J(P_bC) = 20.82$ Hz, C_7), 57.68 (dd, $^1J(P_bC) = 34.01$ Hz, $^2J(P_aC) = 18.37$ Hz, C_1), 117.65 (d, $^3J(P_aC) = 7.86$ Hz, C_{12}), 117.73 (d, $^1J(P_bC) = 58.41$ Hz, C_4), 124.35 (d, $^1J(P_aC) = 46.86$ Hz, C_{10}), 128.91 (d, $^3J(PC) = 11.79$ Hz, C_m), 129.18 (d, $^3J(PC) = 11.71$ Hz, C_m), 130.06 (d, $^1J(PC) = 47.61$ Hz, C_i), 131.12 (d, $^1J(PC) = 48.75$ Hz, C_i), 132.11 (d, $^4J(PC) = 2.87$ Hz, C_p), 132.55 (d, $^4J(PC) = 2.87$ Hz, C_p), 132.57 (d, $^2J(PC) = 12.70$ Hz, C_o), 133.22 (d, $^2J(PC) = 12.62$ Hz, C_o), 146.96 (dd, $^2J(P_aC) = 14.67$ Hz, $^3J(P_bC) = 7.03$ Hz, C_8), 157.64 (dd, $^2J(P_bC) = 5.74$ Hz, $^4J(P_aC) = 0.68$ Hz, C_3), 163.81 (dd, $^2J(P_aC) = 14.10$ Hz, $^4J(P_bC) = 2.50$ Hz, C_9). Anal. Calcd for $C_{24}H_{26}Br_2P_2Pd\cdot H_2O$: C, 43.65; H, 4.24; Br, 24.20. Found: C, 43.72; H, 3.94; Br, 24.13.

Solid-State Preparation of (DPTCT)$PdBr_2$, {$(DMPP)_2$[2 + 2]}-$PdBr_2$, and [$(DMPP)]_2$(*exo*-methylene)]$PdBr_2$. *cis*-$(DMPP)_2PdBr_2$ or *trans*-$(DMPP)_2PdBr_2$ (1.00 g) was sealed in a break-seal ampule under nitrogen and heated in an oven at 140 °C for 30 h. The solid was dissolved in $CDCl_3$ and the solution was filtered. The relative amounts of (DPTCT)$PdBr_2$, the [2 + 2], and *exo*-methylene products were determined to be 1:2:2 by $^{31}P\{^1H\}$ NMR spectroscopy. Slow and careful fractional crystallization from $CHCl_3$/ETOH afforded 64 mg of (DPTCT)$PdBr_2$ as the least soluble product, mp 308−312 °C (dec.). $^{31}P\{^1H\}$ NMR ($CDCl_3$): δ 31.52 (d, $^2J(PP) = 23.42$ Hz, P_a), 94.65 (d, $^2J(PP) = 23.42$ Hz, P_b). ^1H NMR ($CDCl_3$): δ 1.27 (d, $^4J(P_bH) = 1.00$ Hz, 3H, $CH_3(17)$), 1.31 (apparent, t $^4J(P_bH) = {}^4J(H_5CH_3) = 1.20$ Hz, 3H, $CH_3(18)$), 1.42 (d, $^4J(P_aH) = 1.00$ Hz, 3H, $CH_3(14)$), 1.62 (s, 3H, $CH_3(16)$), 2.07 (dd, $^4J(P_aH) = 2.25$ Hz, $^4J(H_1CH_3) = 1.25$ Hz, 3H, $CH_3(13)$), 2.28 (d, $^4J(H_2CH_3) = 1.50$ Hz, 3H, $CH_3(15)$), 2.30 (apparent dt, $^3J(P_bH) = 1.50$ Hz, $^4J(H_5H_6) = {}^3J(H_4H_5) = 0.90$ Hz, 1H, H_5), 2.57 (dddd, $^3J(P_aH) = 24.49$ Hz, $^3J(P_bH) = 21.87$ Hz, $^3J(H_3H_4) = 8.13$ Hz, $^3J(H_4H_5) = 0.90$ Hz, 1H, H_4), 3.14 (ddd, $^2J(P_aH_3) = 13.00$ Hz, $^3J(H_3H_4) = 8.13$ Hz, $^4J(P_bH_3) = 2.50$ Hz, 1H, H_3), 3.68 (dd, $^2J(P_bH_6) = 2.00$ Hz, $^4J(H_5H_6) = 0.90$ Hz, 1H, H_6), 5.36 (q, $^4J(H_2CH_3(15)) = 1.50$ Hz, 1H, H_2), 6.27 (dq, $^2J(P_aH_1) = 26.99$ Hz, $^4J(H_1CH_3(13) = 1.25$ Hz, 1H, H_1), 7.2−8.1 (m, 10H, Ph). Limited solubility precluded obtention of a $^{13}C\{^1H\}$ NMR spectrum. Anal. Calcd for $C_{30}H_{34}Br_2P_2Pd$: C, 49.87; H, 4.70; Br, 22.12. Found: C, 49.62; H, 4.28; Br, 21.91. From the next fraction was obtained 218 mg of {$(DMPP)_2$[2 + 2]}$PdBr_2\cdot 0.75\ H_2O$,

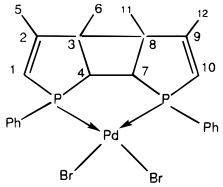

mp 276−280 °C (dec.). $^{31}P\{^1H\}$ NMR ($CDCl_3$): δ 108.76 (s). ^1H NMR ($CDCl_3$): δ 1.53 (s, 6H, $CH_3(6, 11)$), 2.01 (T, $|^4J(PH) + {}^6J(PH)| = 2.15$ Hz, 6H, $CH_3(5,12)$), 2.92 (AA′XX′, $^3J(HH) = 14.00$ Hz, $^2J(PH) = 22.29$ Hz, $^3J(PH) = 1.30$ Hz, $^2J(PP) = 26.87$ Hz, 2H, HC_4C_7), 6.32 (AA′XX′, $^2J(PH) = 28.00$ Hz, $^4J(PH) = 1.00$ Hz, $^2J(PP) = 26.87$ Hz, 2H, HC_1C_{10}), 7.4−7.8 (m, 10H, Ph). H_2O was detected in the ^1H NMR spectrum in approximately the correct ratio. $^{13}C\{^1H\}$ NMR ($CDCl_3$): δ 18.12 (T, $|^3J(PC) + {}^4J(PC)| = 14.08$ Hz, $C_{6,11}$), 22.74 (T, $|^3J(PC) + {}^5J(PC)| = 6.29$ Hz, $C_{5,12}$), 53.43 (T, $|^1J(PC) + {}^3J(PC)| = 46.39$ Hz, $C_{4,7}$), 67.93 (T, $|^2J(PC) + {}^3J(PC)| = 9.05$ Hz, $C_{3,8}$), 122.79 (AXX′, $^1J(PC) = 51.41$ Hz, $^3J(PC) = 0.25$ Hz, $^2J(PP) = 26.87$ Hz, $C_{1,10}$), 128.70 (T, $|^3J(PC) + {}^5J(PC)| = 11.69$ Hz, C_m), 131.91 (s, C_p), 132.81 (T, $|^2J(PC) + {}^4J(PC)| = 12.19$ Hz, C_o), 132.91 (apparent dd, $^1J(PC) = 80.01$ Hz, $^3J(PC) = 12.6$ Hz, C_i), 160.18 (T, $|^2J(PC) + {}^4J((PC)| = 9.55$ Hz, $C_{2,8}$). Anal. Calcd for $C_{24}H_{26}Br_2P_2Pd\cdot 0.75\ H_2O$: C, 43.95; H, 4.19; Br, 24.39. Found: C, 43.62; H, 3.89; Br, 24.58. Finally, 189 mg of [$(DMPP)_2$(*exo*-methylene)]$_2PdBr_2$ was obtained as the most soluble product.

C. Kinetic Studies. Solutions of *cis*-$(DMPP)_2PdCl_2$ (0.0036, 0.0072, and 0.0144M) in 1,1,2,2-tetrachloroethane solvent were heated at gentle reflux in a two-neck round-bottom flask fitted with a rubber septum, a reflux condenser, and an N_2 inlet and outlet. Aliquots were removed periodically, and their contents were determined by $^{31}P\{^1H\}$ NMR spectroscopy at 121.65 MHz on a G.E. GN-300 NMR spectrometer, with 60° pulses and duty cycles of 5 s which is approximately 5 times the longest T_1.

D. Numerical Simulation of Reaction Kinetics. The kinetics of the reaction were simulated by numerically integrating the differential

Table 1. Abridged Summary of Data Collection Parameters for (DPTCT)$PdCl_2$ (**1**), *trans*-$(DMPP)_2PdBr_2$ (**2**), *trans*-$(DMPP)_2PdI_2$ (**3**), [$(DMPP)_2$(*exo*-methylene)]$PdBr_2$ (**4**), and {$(DMPP)_2$[2 + 2]}$PdBr_2$ (**5**)[a]

	1·0.5CH_3OH·H_2O	**2**	**3**	**4**·H_2O	**5**·0.75H_2O
formula	$C_{30}H_{34}Cl_2P_2Pd$	$C_{24}H_{26}Br_2P_2Pd$	$C_{24}H_{26}I_2P_2Pd$	$C_{24}H_{26}Br_2P_2Pd$	$C_{24}H_{26}Br_2P_2Pd$
fw	667.58	642.6	736.6	642.6	642.6
color and habit	yellow plates	orange cubes	red-orange plates	yellow prisms	yellow plates
space group	$P2_12_12_1$	$P2_1/c$	$P\bar{1}$	$P2_1/n$	$P2_1/c$
crystal size, mm	0.26 × 0.32 × 0.38	0.18 × 0.18 × 0.35	0.2 × 0.1 × 0.4	0.2 × 0.2 × 0.4	0.02 × 0.4x0.1
a, Å	15.532(3)	10.158(3)	9.205(1)	10.72(1)	13.090(2)
b, Å	19.401(4)	14.876(4)	11.023(1)	16.929(1)	17.637(2)
c, Å	9.910(2)	16.829(5)	13.833(1)	14.675(1)	21.834(2)
α, deg			101.15(1)		
β, deg		104.25(2)	98.82(1)	97.86(1)	100.51(1)
γ, deg			105.30(1)		
V, Å^3	2986.2	2464.7	1296.9(2)	2638.2(3)	4956.5(10)
Z	2	4	2	4	4
d(calc), g/cm^3	1.490	1.732	1.886	1.663	1.738
linear abs coeff, cm^{-1}	9.229	40.924	32.28	38.67	41.13
2*θ* range, deg	2−25	2−24	3.5−45	2−45	3.5−45
no. of obs reflcns	2525 ($I > 3\sigma(I)$)	2770 ($I > 3\sigma(I)$)	2672 ($F > 4\sigma(F)$)	2159 ($F > 4\sigma(F)$)	2729 ($F > 5\sigma(F)$)
no. of variables	333	261	263	272	271
R,R_w[b]	0.035, 0.057	0.041, 0.053	0.035, 0.045	0.053, 0.064	0.062, 0.075

[a] Data were collected at 298 K using an Enraf-Nonius CAD4-F diffractometer, Mo Kα (λ = 0.709 30 Å) for **1**, a syntex P3 diffractometer, Mo Kα (λ = 0.710 7 Å for **2**; and a Siemens P4, Mo Kα (λ = 0.710 73 Å) for **3**-**5**. [b] For **1** and **2** $R(F) = \sum(|F_o| - |F_c|/\sum F_o|)$, $R_w(F) = [\sum w(|F_o| - F_c|^2/\sum w|F_o|^2]^{1/2}$, $w = 1/\sigma^2(F^2) = \sigma^2$ (counts + $(pI)^2$; for **3**−**5** $R_w(F) = [\sum w(F_o^2 - F_c^2)^2/\sum w(F_o^2)^2]^{1/2}$.

rate laws (*vide infra*). The integration was carried out using a fourth order Gear integrator with a constant time step of 0.02 h for 2250 time steps (about 45 h). This procedure conserved the material balance to better than 1 part in 10^8. The routine was adjusted to interpolate between integration points to obtain calculated mole fractions of each of the reaction species for the same time points at which the experimental data were collected. For a given trial set of rate constants, the summed square deviation (variance) of the computed data relative to the experimental data was accumulated, and then the rate constants were iteratively adjusted until the variance had been minimized. All experimental data were given equal weighing in this fitting procedure.

E. X-ray Data Collection and Processing. Bright yellow crystals of (DPTCT)$PdCl_2$ were obtained from CH_3OH/H_2O, orange crystals of *trans*-$(DMPP)_2PdBr_2$ were obtained from benzene, dark red-orange crystals of *trans*-$(DMPP)_2PdI_2$ were obtained from chloroform, and yellow crystals of [$(DMPP)_2$(*exo*-methylene)]$PdBr_2$ and {$(DMPP)_2$[2 + 2]}$PdBr_2$ were obtained from chloroform/ethanol. Crystal data and details of the data collection are given in Table 1. In all cases, single crystals were cut from clusters of crystals. Systematic searches in reciprocal space with an Enraf-Nonius CAD4-F diffractometer showed that the crystals of (DPTCT)$PdCl_2$ belong to the orthorhombic system and for *trans*-$(DMPP)_2PdBr_2$ data collected on a Syntex P3 diffractometer showed that the crystals belonged to the monoclinic system, while for *trans*-$(DMPP)_2PdI_2$, [$(DMPP)_2$(*exo*-methylene)]$PdBr_2$ and{$(DMPP)_2$-[2 + 2]}$PdBr_2$ data collected on a Siemens P4 diffractometer showed that the crystals belong to the triclinic, monoclinic, and monoclinic systems respectively. Quantitative data for the first two compounds were obtained at room temperature in the $\theta-2\theta$ mode. The resulting data sets were transferred to a VAX computer, and for all subsequent calculations, the Molen package[18] was used for (DPTCT)$PdCl_2$ and SHELXTL Plus[19] was used for *trans*-$(DMPP)_2PdBr_2$. Three standard reflections measured every 1 h during the entire data collection periods showed no significant trends. The raw data were converted to intensities and corrected for Lorentz, polarization, and absorption effects within SHELXTL Plus for *trans*-$(DMPP)_2PdBr_2$ by the Gaussian method. For (DPTCT)$PdCl_2$, no absorption corrections were applied as the absorption coefficient is small. The structures were solved by the heavy-atom method. For (DPTCT)$PdCl_2$ the CH_3OH molecule is disordered over two positions related by a 2-fold crystallographic axis superimposing the C and O atoms; this disorder was treated by affecting to the C/O position a mixed form factor of 50% C + 50% O. After refinement of the heavy atoms, difference Fourier maps revealed maximas of residual electronic density close to positions expected for hydrogen atoms. They were introduced in the structure calculations by their computed coordinates (CH = 0.95 Å) with isotropic temperature factors such as $B(H) = 1.3B_{eqv}(C)$ Å^3 but were not refined. For (DPTCT)$PdCl_2$ the absolute structure was determined by comparing $+x$, $+y$, $+z$ and $-x$, $-y$, $-z$ refinements (Flack absolute structure parameter $X = 0.37(7)$).[20] Solutions were obtained with full least-squares refinements with weighting schemes given in Table 1. Final difference maps revealed no significant maxima. The scattering factor coefficients and anomalous dispersion coefficients come respectively from parts a and b of ref 21. The *trans*-$(DMPP)_2PdI_2$, [$(DMPP)_2$(*exo*-methylene)]$PdBr_2$, and {-$(DMPP)_2$[2 + 2]}$PdBr_2$ crystals were coated with epoxy, mounted on glass fibers and placed on a Siemens P4 diffractometer. Two check reflections monitored every 100 reflections, showed random (<2%) variation during the data collection. Unit cell parameters were determined by least-squares refinement of 24 reflections. The data were corrected for Lorentz, polarization, and absorption effects (using an empirical model derived from azimuthal data collections). Scattering factors and corrections for anomalous dispersion were taken from a standard source.[22] Calculations were performed with the Siemens SHELXTL Plus version 4.0 software package on a personal computer. The structures were solved by direct methods. Anisotropic thermal parameters were assigned to all non-hydrogen atoms. Hydrogen atoms were refined at calculated positions with a riding model in which the C−H vector was fixed at 0.96 Å. For {$(DMPP)_2$[2 + 2]}$PdBr_2$ anisotropic thermal parameters were assigned to palladium, phosphorus, and bromine atoms. All other atoms were refined with isotropic thermal parameters. Hydrogen atoms were added to appropriate atoms excluding the solvate and were refined at calculated positions with a riding model as above. One phenyl ring (C37 to C42) was modeled as a rigid group. There was disordered solvent equivalent to three-fourths of a water molecule occupying two sites. Selected bond lengths and angles are given in Tables 2 and 4−6.

Results and Discussion

$(DMPP)_2PdX_2$ complexes are present in solution as equilibrium mixtures of the *cis*- and *trans*-isomers.[17,23] These equilibria are solvent and temperature dependent such that the generally thermodynamically more stable *cis* isomers are stabilized by

(18) *Molen, An Interactive Structure Solution Procedure*; Enraf-Nonius: Delft, The Netherlands, 1990.
(19) Sheldrick, G. M. *SHELXTL User Manual*; Nicolet: Madison, WI, 1986.
(20) Flack, H. D. *Acta Crystallogr.* **1984**, *A41*, 500.
(21) Cromer, D. T.; Waber, J. T. I*nternational Tables for X-ray Crystallography;* Kynoch: Birmingham, England, 1974; Vol. IV, (a) Table 2.2b; (b) Table 2.3.1.
(22) *International Tables for X-ray Crystallography*; Reidel: Boston, MA, 1992; Vol. C.
(23) MacDougall, J. J.; Mathey, F.; Nelson, J. H. *Inorg. Chem.* **1980**, *19*, 1400.

Table 2. Selected Bond Lengths (Å) and Angles (deg) for *trans*-$(DMPP)_2PdBr_2$, *trans*-$(DMPP)_2PdI_2$ and *cis*-$(DMPP)_2PdCl_2$[17]

Bond Lengths

trans-$(DMPP)_2PdBr_2$		*trans*-$(DMPP)_2PdI_2$		*cis*-$(DMPP)_2PdCl_2$	
Pd−Br1	2.4334(8)	Pd1−I1	2.603(1)	Pd−Cl1	2.350(3)
Pd−Br2	2.4349(8)	Pd1−I2	2.609(1)	Pd−Cl2	2.356(3)
Pd−P1	2.319(2)	Pd1−P1	2.324(2)	Pd−P1	2.243(3)
Pd−P2	2.313(2)	Pd1−P2	2.312(2)	Pd−P2	2.238(2)
P1−C1	1.793(6)	P1−C1	1.801(10)	P1−C11	1.799(9)
P1−C4	1.782(6)	P1−C4	1.804(7)	P1−C14	1.791(9)
P2−C13	1.790(6)	P2−C13	1.790(9)	P2−C21	1.793(1)
P2−C16	1.789(6)	P2−C16	1.788(9)	P2−C24	1.790

Bond Angles

trans-$(DMPP)_2PdBr_2$		*trans*-$(DMPP)_2PdI_2$		*cis*-$(DMPP)_2PdCl_2$	
Br1−Pd−Br2	177.57(3)	I1−Pd1−I2	167.8(1)	Cl1−Pd−Cl2	91.3(1)
Br1−Pd−P1	89.08(5)	I1−Pd1−P1	91.2(1)	C12−Pd−P1	178.6(1)
Br1−Pd−P2	90.20(4)	I1−Pd1−P2	89.9(1)	Cl1−Pd−P1	88.90(9)
Br2−Pd−P1	90.81(4)	I2−Pd1−P1	90.3(1)	Cl2−Pd−P2	86.0(1)
Br2−Pd−P2	90.05(4)	I2−Pd1−P2	89.7(1)	Cl1−Pd−P2	172.3(1)
P1−Pd−P2	176.80(6)	P1−Pd1−P2	174.8(1)	P1−Pd−P2	93.43(9)
C1−P1−C4	91.9(3)	C1−P1−C4	91.0(4)	C11−P1−C14	92.7(5)
C13−P2−C16	91.5(3)	C13−P1−C16	92.0(5)	C21−P2−C24	91.8(2)

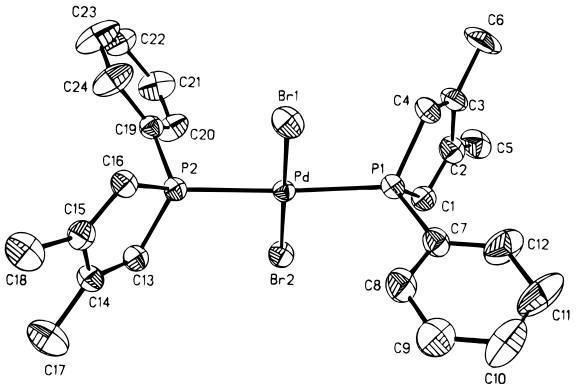

Figure 1. ORTEP Drawing of *trans*-$(DMPP)_2PdBr_2$ showing the atom numbering scheme (50% probability ellipsoids). Hydrogen atoms are omitted.

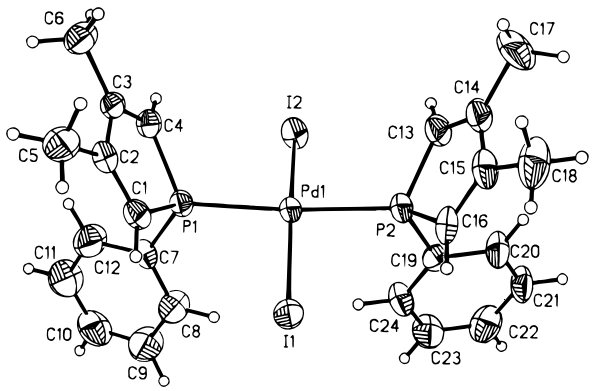

Figure 2. Perspective drawing of *trans*-$(DMPP)_2PdI_2$ showing the atom numbering scheme (50% probability ellipsoids). Hydrogen atoms have an arbitrary radius of 0.1 Å.

high dipole moment solvents and the *trans* isomer population increases with increasing temperature and increasing ligand steric bulk. Thus, $(DMPP)_2PdCl_2$ is wholly *cis*; $(DMPP)_2PdBr_2$, a 0.51:1.00 mixture of the *trans*- and *cis*-isomers; and $(DMPP)_2PdI_2$, wholly *trans* in $CDCl_3$ at ambient temperature as shown by ^1H, $^{13}C\{^1H\}$, and $^{31}P\{^1H\}$ NMR spectroscopy.[17] Whereas, the *cis*- and *trans*-isomers are both often easily isolated for the robust $(R_3P)_2PtX_2$ complexes,[14,24,25] in only a few cases[14,26,27] have both the *cis*- and *trans*-isomers been isolated for the more labile $(R_3P)_2PdX_2$ complexes. Thus, we have completely characterized the *cis*- and *trans*-isomers of $(DMPP)_2PdBr_2$. The *cis*-isomer was isolated from an acetone/water mixture as yellow needles and the *trans*-isomer from benzene as orange cubes. We were only able to obtain X-ray quality crystals for the *trans*-isomer, and its structure is shown in Figure 1. We were also able to obtain crystals of the analogous *trans*-$(DMPP)_2PdI_2$, and its structure is shown in Figure 2. Both complexes crystallize as discrete molecular entities with no unusual intermolecular contacts. The molecules possess near, but not exact, C_{2h} symmetry. The PdBr (2.4334(8), 2.4349(8) Å), PdI (2.603(1), 2.609(1) Å), PdP (2.319(2), 2.313(2) Å), and (2.324(2), 2.312(2) Å) distances (Table 2) are not identical. The palladium coordination geometries are essentially planar as the sums of the bond angles around the metal are 360.14(5)° and 361.1(1)° and the dihedral angles between the X1−Pd−P1 and X2−Pd−P2 planes are small (1.2 and 13.2°), respectively. By way of comparison, for *cis*-$(DMPP)_2PdCl_2$ with approximate C_2 symmetry, the PdCl (2.350(3), 2.356(3) Å) and PdP (2.243(3), 2.238(2) Å) distances (Table 2) show similar differences. This complex exhibits a small degree of tetrahedral distortion as the sum of the bond angles around palladium is 359.63(10)° and the dihedral angle between the Cl−Pd−Cl and P−Pd−P planes is 7.2°.

Dissolution of either *cis*- or *trans*-$(DMPP)_2PdBr_2$ in $CDCl_3$ forms an equilibrium mixture of the two isomers as the ^1H, $^{13}C\{^1H\}$, and $^{31}P\{^1H\}$ NMR spectra of both isomers are identical to those reported previously.[17] The two isomers exhibit essentially the same melting points (*trans*, 234−236 °C; *cis*, 229−231 °C), suggesting that they isomerize in the solid state as well. Solid-state isomerizations of L_2PtX_2 complexes are well-documented.[28−33]

Cis- and *trans*-$(DMPP)_2PdBr_2$ may be distinguished by infrared spectroscopy as follows. For the C_2 symmetry *cis*-isomer, two υ_{PdP} and two υ_{PdBr} vibrations are expected and observed. For the C_{2h} symmetry *trans*-isomer, only one υ_{PdP} and one υ_{PdBr} vibration is expected and observed (see Experimental Section). They may also be distinguished by CP/MAS $^{31}P\{^1H\}$ NMR spectroscopy.[34−36]

(24) Chatt, J.; Wilkins, R. G. *J. Chem. Soc.* **1952**, *273*, 4300.
(25) Chatt, J.; Wilkins, R. G. *J. Chem. Soc.* **1956**, 525.
(26) Cheney, A. J.; Mann, B. E.; Shaw, B. L.; Slade, R. M. *J. Chem. Soc. (A)* **1971**, 3833.
(27) Allen, E. A.; Wilkinson, W. *J. Inorg. Nucl. Chem.* **1974**, *36*, 1663.
(28) Ellis, R.; Weil, T. A.; Orchin, M. *J. Am. Chem. Soc.* **1970**, *92*, 1078.

Table 3. Solution and CP/MAS ^{31}P NMR Data for $(DMPP)_2PdX_2$ Complexes[a]

X	$\delta(^{31}P)(CDCl_3)$	$\delta_{iso}(^{31}P)$	δ_{11}	δ_{22}	δ_{33}
Cl	26.4 (*cis*)	28	60	44	−18
Br	24.2 (*cis*)	30,26[b]	62	36	−18
	17.5 (*trans*)	19[c]	46	26	−12
I	9.5 (*trans*)	11	40	19	−25

[a] Chemical shifts are reported with respect to 85% H_3PO_4. Errors in the principal components are ±5 ppm unless indicated otherwise. [b] Two sites with tensor components equal within ±10 ppm. [c] $^2J(P,P) = 540 \pm 40$ Hz.

CP/MAS ^{31}P{^{1}H} NMR Spectroscopy. The phosphorus chemical shift tensors obtained from analysis of ^{31}P MAS and static NMR spectra of *cis*- and *trans*-complexes of DMPP with palladium halides are summarized in Table 3. For the bromo and iodo derivatives, relatively broad peaks ($\Delta\upsilon \approx 300-600$ Hz) were observed due to incomplete averaging of the dipolar interaction involving ^{31}P and the quadrupolar nuclei present in these complexes (e.g., $^{79/81}$Br and ^{127}I). From the data presented in Table 3, it is clear that the difference in isotropic chemical shifts between the *cis*- and *trans*-arrangements of phosphine ligands results mainly from variations in the least and intermediate shielded principal components, δ_{11} and δ_{22}, which are more shielded in the latter by about 10 ppm (cf. *cis*- and *trans*-$(DMPP)_2PdBr_2$). It has been found that differences in isotropic chemical shifts for phosphorus nuclei in different polymorphs or crystallographically nonequivalent positions may be 10 ppm or more; even larger differences in the principal components have been noted.[37] Such large differences in the phosphorus chemical shift with subtle structural variations make if difficult to discuss the small changes in chemical shift with the geometrical arrangement of phosphine ligands.

For *cis*-$(DMPP)_2PdCl_2$, two resonances at 28 and 27 ppm were observed in the ^{31}P CP/MAS NMR spectrum obtained at 9.4 T (see insert Figure 3). Note, that these values are different from those reported earlier.[34] On first sight, the observation of two resonances is consistent with the crystal structure of this compound, as the two phosphine ligands are crystallographically nonequivalent.[17] However, a detailed investigation revealed that the peak-to-peak separation between these resonances is dependent on the sample spinning frequency. The maximum peak splitting observed at $B_o = 9.4$ T was 165 Hz when the MAS rate was 3.0 kHz. In the discussion that follows, it is necessary to define crystallographic and magnetic equivalence. Also, it is important to recognize how the solid-state ^{31}P MAS NMR

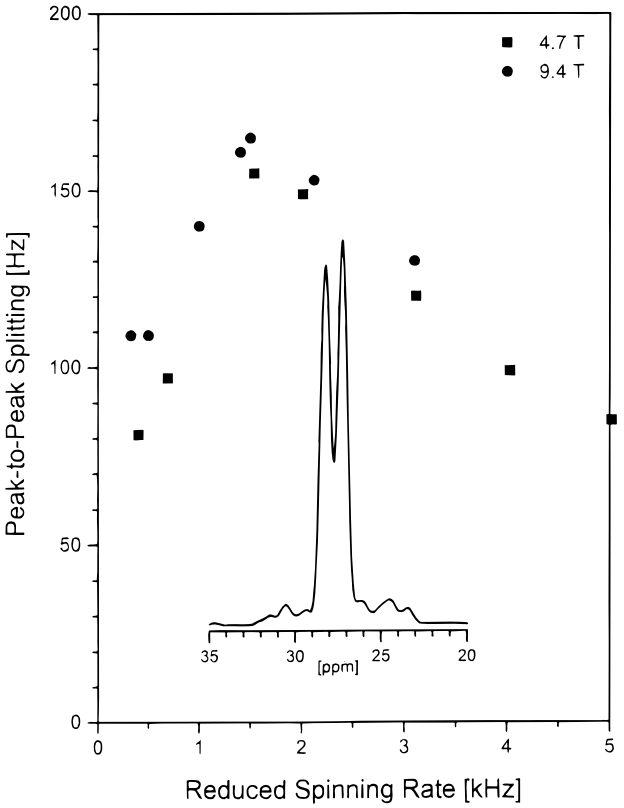

Figure 3. Dependence of the peak-to-peak splitting in the ^{31}P CP/MAS NMR spectrum of *cis*-$(DMPP)_2PdCl_2$ on the spinning rate and the strength of the external magnetic field. For the measurements at 9.4 T, a reduced spinning rate was used; i.e., the rates were divided by 2. The insert shows the isotropic region of the ^{31}P CP/MAS NMR spectrum obtained at 9.4 T and a spinning rate of 2.8 kHz. Note the presence of ^{105}Pd satellites.

spectra of mononuclear bisphosphine complexes will differ depending on whether or not two phosphines are crystallographically or magnetically equivalent. Two phosphine ligands are crystallographically equivalent if they are related by a symmetry element of the space group. Thus, crystallographically equivalent phosphine ligands will have identical isotropic chemical shifts. As well, the principal components of their respective chemical shift tensors will be of identical magnitude. However, the orientations of the two chemical shift tensors will not, in general, be coincident. In order to be magnetically equivalent, the nuclei must be crystallographically equivalent *and* the orientations of the principal axes of both tensors must coincide. This requirement is generally only fulfilled if both phosphine ligands are related by a center of inversion or a translation. Only for a *trans*-arrangement of ligands is a center of inversion possible at the metal center. For an isolated pair of magnetically equivalent nuclei, theory predicts the MAS line shapes to be independent of the sample spinning frequency.[38] For *cis*-complexes, the indirect spin−spin coupling between the two ^{31}P nuclei is in most cases smaller than 50 Hz and hence smaller than the typical line widths in ^{31}P CP/MAS NMR spectra.[39] However, the direct dipolar coupling for typical P−P distances is still sizable (200−400 Hz). Depending on the relative orientations of the two CS tensors, the direct dipolar interaction may become homogeneous. This in turn may result

(29) Kukushkin, Y. N.; Budanova, V. F.; Sedove, G. N.; Pogareva, V. G.; Fadeev, Y. V.; Soboleva, M. S. *Zh. Neorg. Khim*, **1976**, *21*, 1265; *Russ. J. Inorg. Chem. (Engl. Transl.)* **1976**, *21*, 689.
(30) Sedova, G. N.; Demchenko, L. N. *Zh. Neorg. Khim.* **1981**, 26, 435; *Russ. J. Inorg. Chem. (Engl. Transl.)* **1981**, *26*, 234.
(31) Kukushkin, Y. N.; Budanova, V. F.; Sedova, G. N.; Pogareva, V. G. *Zh. Neorg. Khim.* **1977**, *22*, 1305; *Russ. J. Inorg. Chem. (Engl. Transl.)* **1977**, *22*, 710.
(32) Kukushkin, Y. N.; Sedova, G. N.; Antonov, P. G.; Mitronina, L. N. *Zh. Neorg. Khim.* **1977**, *22*, 2785; *Russ. J. Inorg. Chem. (Engl. Transl.)* **1977**, *22*, 1512.
(33) Andronov, E. A.; Kukushkin, Y. N.; Lukicheva, T. M.; Kunovalou, L. V.; Bakhireva, S. I.; Postnikova, E. S. *Zh. Neorg. Khim.* **1976**, *21*, 2443; *Russ. J. Inorg. Chem. (Engl. Transl.)* **1976**, *21*, 1343.
(34) Nelson, J. H.; Rahn, J. A.; Bearden, W. H. *Inorg. Chem.* **1987**, *26*, 2192.
(35) Rahn, J. A.; O'Donnell, D. J.; Palmer, A. R.; Nelson, J. H. *Inorg. Chem.* **1989**, *28*, 3631.
(36) Rahn, J. A.; Baltusis, L.; Nelson, J. H. *Inorg. Chem.* **1990**, *29*, 750.
(37) (a) Naito, A.; Sastry, D. L.; McDowell, C. A. *Chem. Phys. Lett.* **1985**, *115*, 19. (b) Power, W. P.; Lumsden, M. D.; Wasylishen, R. E. *J. Am. Chem. Soc.* **1991**, *113*, 8257. (c) Jarrett, P. S.; Sadler, P. J. *Inorg. Chem.* **1991**, *30*, 2098. (d) Lindner, E.; Fawzi, R.; Mayer, H. A.; Eichele, K.; Hiller, W. *Organometallics* **1992**, *11*, 1033. e) Szalontai, G.; Bakos, J.; Aime, S.; Gobetto, R. *J. Organomet. Chem.* **1993**, *463*, 223.
(38) (a) Wu, G.; Wasylishen, R. E. *Inorg. Chem.* **1994**, *33*, 2774. (b) Wu, G.; Wasylishen, R. E. *J. Chem. Phys.* **1993**, *99*, 6391. (c) Wu, G.; Wasylishen, R. E. *J. Chem. Phys.* **1993**, *98*, 6138. (d) Eichele, K.; Wu. G.; Wasylishen, R. E. *J. Magn. Reson., Ser. A* **1993**, *101*, 156.
(39) Pregosin, P. S.; Kunz, R. W. In *NMR Basic Principles and Progress*; Diehl, P., Fluck, E., Kosfeld, R., Eds.; Springer-Verlag: Berlin, 1976; Vol. 16.

in the observation of spinning-rate dependent splittings. As previously shown,[38a] in order to determine whether or not two nuclei are crystallographically equivalent, it is advantageous to study the spinning-rate dependence of the splittings at different external applied magnetic fields. If the two nuclei are crystallographically equivalent, the spinning-rate dependence of the splittings is independent of the reduced sample spinning frequency, ω_R^{red}. Here, we define $\omega_R^{red} = \omega_R\ (4.7/B_o)$, where ω_R is the sample spinning frequency measured at B_o (in tesla). To determine whether or not the two phosphorus nuclei of *cis*-$(DMPP)_2PdCl_2$ are crystallographically equivalent, the spinning-rate dependence of this splitting was studied at 9.4 T. Using a reduced spinning rate, the spinning-rate dependencies at both fields are superimposable and imply that the two phosphorus nuclei are crystallographically equivalent within experimental error. Note, however, that this criterium for crystallographic equivalence only means that they are equivalent within experimental error, as only the establishment of nonequivalence is unambigous.

The two samples of *cis*-$(DMPP)_2PdCl_2$ examined by CP/MAS ^{31}P NMR spectroscopy are polymorphic. That examined earlier[34] was obtained from CH_3OH solution as yellow monoclinic crystals,[17] space group C_c, with a unit cell of the following dimensions: $a = 10.427(4)$ Å, $b = 15.070(6)$ Å, $c = 15.910(6)$ Å, $\beta = 92.88(2)°$, $Z = 4$. Those investigated in this work were obtained from benzene as yellow monoclinic crystals, space group $P2_1/c$, with a unit cell of the following dimensions: $a = 11.425(2)$ Å, $b = 8.687(1)$ Å, $c = 26.212(4)$ Å, $\beta = 100.64(1)°$, $Z = 4$. Structure refinement of these latter crystals did not proceed below $R = 0.107$ due to severe disorder of both phosphole ligands.

The ^{31}P CP/MAS NMR spectrum of *cis*-$(DMPP)_2PdCl_2$ also revealed some interesting features as small satellites (see Figure 3). We attribute these satellites to dipolar and indirect spin−spin coupling of ^{31}P to ^{105}Pd ($I = {}^5/_2$, 22.3%). Due to the complex nature of the uncoupled central peak (i.e., the spinning-frequency dependent splitting), no attempt has been made to analyze this effect. However, this appears to be the first report of spin−spin coupling involving ^{105}Pd.

For *trans*-$(DMPP)_2PdBr_2$, only one broad peak was discernable in the ^{31}P CP/MAS NMR spectrum but with some interesting features in the spinning side bands; i.e., their shape differs from the isotropic peak and indicates strong coupling effects. The crystal structure shows two nonequivalent phosphole ligands. A two-dimensional *J*-resolved spectrum[40] revealed $J(PP) \approx 540 \pm 40$ Hz, comparable to other values of $^2J(PP)$ *trans*-coupling constants in palladium phosphine complexes[39], hence establishing the *trans*-geometry of this compound. The 2D *J*-resolved spectrum is shown in Figure 4.

Thermolyses Reactions. Both *cis*-$(DMPP)_2PdCl_2$ and *cis*- or *trans*-$(DMPP)_2PdBr_2$ undergo thermal coupling reactions of their coordinated phospholes, yielding four products, while thermolysis of *trans*-$(DMPP)_2PdI_2$ gives none of these products. These products are a [2 + 2] cycloaddition product, A; a [4 + 2] cycloaddition product, B, a third compound, C, in which a carbon−carbon bond is formed between carbons 1 and 1′ and a hydrogen is transferred to carbon 2 from the methyl group on carbon 2′, which is referred to as the *exo*-methylene product; and a fourth compound, D, that is possibly formed by the following sequence of reactions: intermolecular *endo*-[4 + 2] cyclodimerization followed by phosphinidene elimination and then intramolecular *exo*-[4 + 2] cycloaddition to another phosphole to give a diphosphatetracyclotetradecatriene referred to as DPTCT (see Scheme 1).

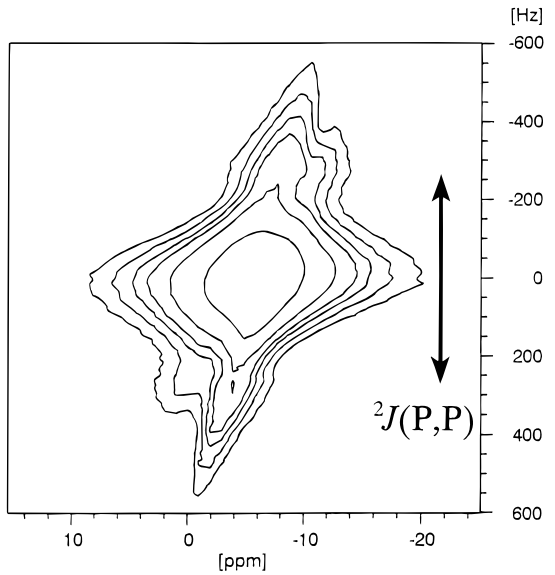

Figure 4. Isotropic region of the 2D homonuclear *J*-resolved ^{31}P CP/MAS NMR spectrum of *trans*-$(DMPP)_2PdBr_2$, obtained at 4.7 T and a spinning rate of 1.8 kHz. The time increment in F1 was synchronized with the sample spinning frequency. The $^2J(PP)$ coupling constant is 540 ± 40 Hz.

Scheme 1

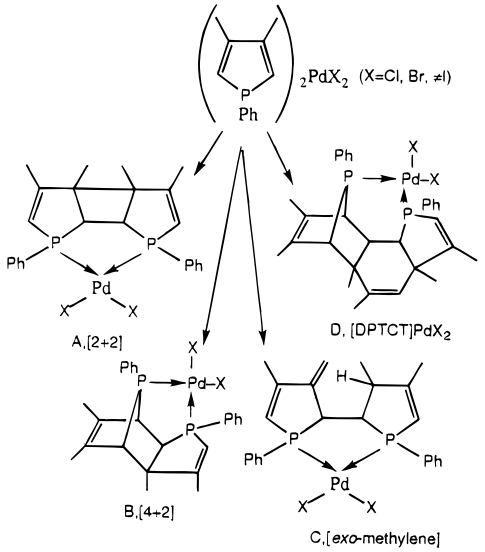

This is in contrast to the thermolyses of *cis*-$(DMPP)_2PtX_2$, where only the platinum analogues of A−C were formed and A and B were ultimately converted to C.[2]

X-ray crystal structures were obtained for an example of three of these compound types. Figures 5 and 6 show the structures of the [2 + 2] cycloaddition product and the *exo*-methylene product, respectively, formed from the thermolysis of *trans*-$(DMPP)_2PdBr_2$, and Figure 7 shows the structure of [DPTCT]-$PdCl_2$ formed from the thermolysis of *cis*-$(DMPP)_2PdCl_2$. Tables 4−6 list relevant bond distances and bond angles. Each of the compounds crystallizes as discrete molecular entities with no unusual intermolecular contacts. The coordination geometry about palladium in each compound is essentially planar as the sums of the bond angles around palladium are very near 360°. The metrical parameters for the analogous palladium and platinum compounds are very similar, yet their chemical reactivities are quite different. The Pd−P bond distances in the [2 + 2] product are slightly different (2.238(5), 2.224(8) Å); they are equal in the *exo*-methylene product (2.219(3), 2.213(4) Å) and in both cases are considerably shorter than those in *trans*-$(DMPP)_2PdBr_2$ (2.319(2), 2.313(2) Å).

(40) Wu, G.; Wasylishen, R. E. *Organometallics* **1992**, *11*, 3242.

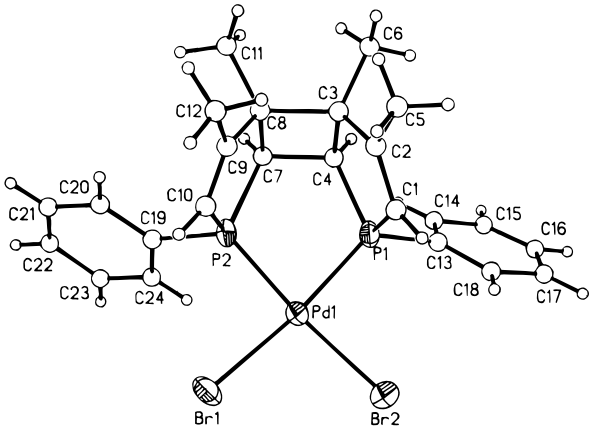

Figure 5. Perspective drawing of $\{(DMPP)_2[2 + 2]\}PdBr_2$ showing the atom numbering scheme (50% probability ellipsoids). Hydrogen atoms have an arbitrary radius of 0.1 Å.

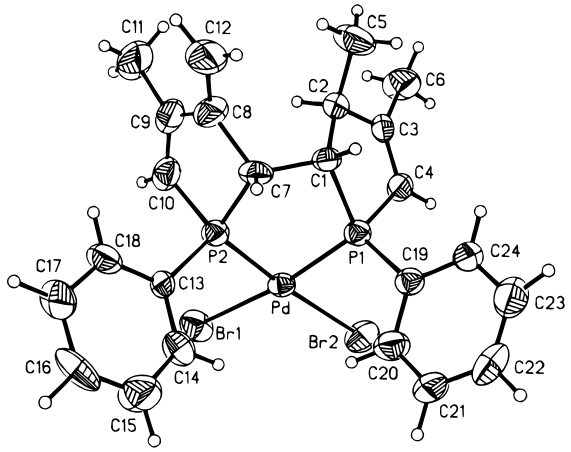

Figure 6. Perspective drawing of $[(DMPP)_2(exo\text{-methylene})]PdBr_2$ showing the atom numbering scheme (50% probability ellipsoids). Hydrogen atoms have an arbitrary radius of 0.1 Å.

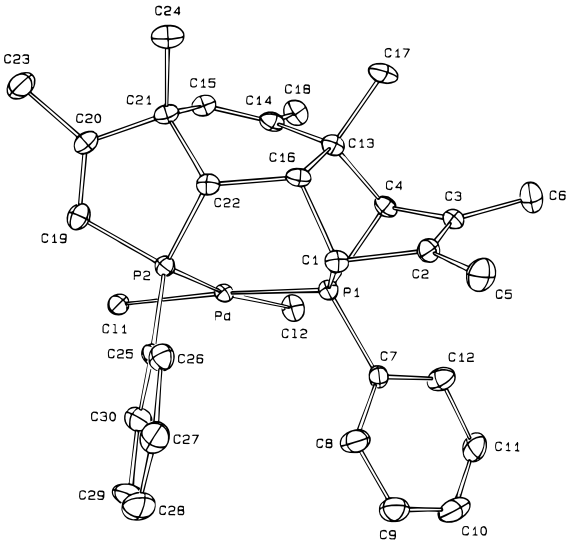

Figure 7. ORTEP drawing of $(DPTCT)PdCl_2$ showing the atom numbering scheme (50% probability ellipsoids). Hydrogen atoms are omitted.

For $(DPTCT)PdCl_2$ there is some tetrahedral distortion as the dihedral angle formed between the P−Pd−P and Cl−Pd−Cl planes is 6.1(4)°. The Pd−P distances (2.208(2), 2.218(2) Å) are shorter than those in *cis*-$(DMPP)_2PdCl_2$ (2.243(3), 2.238(2) Å) as a result of the formation of a six-membered chelate ring. The Pd−Cl distances (2.381(1), 2.369(2) Å) are slightly lengthened relative to those in *cis*-$(DMPP)_2PdCl_2$ (2.350(3), 2.356(3) Å). The C2−C3 (1.33(1) Å), C14−C15 (1.33(1) Å), and C19−C20 (1.32(1) Å) distances are all in the range expected for double bonds. The final reaction step in the formation of $(DPTCT)PdCl_2$ is diastereospecific, forming only a racemic mixture of the *exo*-diastereomer, as expected for an intramolecular [4 + 2] cycloaddition between a metal-coordinated diene and dienophile.[41]

Table 4. Selected Bond Lengths (Å) and Angles (deg) for $\{(DMPP)_2[2 + 2]\}PdBr_2$ and $\{(DMB^tP)_2[2 + 2]\}PtBr_2$[2]

Bond Lengths

$\{(DMPP)_2[2 + 2]\}PdBr_2$		$\{(DMB^tP)_2[2 + 2]\}PtBr_2$	
Pd1−Br1	2.476(2)	Pt−Br1	2.488(1)
Pd1−Br2	2.480(3)	Pt−Br2	2.491(1)
Pd1−P1	2.238(5)	Pt−P1	2.237(8)
Pd1−P2	2.224(8)	Pt−P2	2.244(3)
C1−C2	1.365(27)	C1−C2	1.32(2)
C2−C3	1.507(29)	C2−C3	1.53(2)
C3−C4	1.573(23)	C3−C4	1.55(1)
C3−C8	1.617(25)	C3−C8	1.59(2)
C4−C7	1.521(24)	C4−C7	1.53(1)
C7−C8	1.560(22)	C7−C8	1.54(1)
C8−C9	1.495(25)	C8−C9	1.52(1)
C9−C10	1.299(24)	C9−C10	1.31(1)

Bond Angles

$\{(DMPP)_2[2 + 2]\}PdBr_2$		$\{(DMB^tP)_2[2 + 2]\}PtBr_2$	
Br1−Pd1−Br2	95.3(1)	Br1−Pt−Br2	86.76(5)
Br2−Pd1−P2	90.2(2)	Br1−Pt−P1	92.78(8)
Br1−Pd1−P2	88.6(1)	Br2−Pt−P2	93.94(8)
P1−Pd1−P2	84.8(2)	P1−Pt−P2	86.1(1)
C1−P1−C4	93.8(9)	C1−P1−C4	92.7(5)
C7−P2−C10	91.9(8)	C7−P2−C10	91.9(5)
P1−C1−C2	113.6(16)	P1−C1−C2	113.8(8)
C1−C2−C3	115.8(16)	C1−C2−C3	117(1)
C2−C3−C4	109.2(15)	C2−C3−C4	108.2(9)
C2−C3−C8	116.1(14)	C2−C3−C8	116.9(9)
C4−C3−C8	90.2(12)	C4−C3−C8	89.4(8)
P1−C4−C3	107.4(13)	P1−C4−C3	108.3(7)
P1−C4−C7	113.7(12)	P1−C4−C7	113.8(7)
C3−C4−C7	89.2(12)	C3−C4−C7	90.3(8)
P2−C7−C4	114.01(1)	P2−C7−C4	115.3(7)
P2−C7−C8	107.0(1)	P2−C7−C8	109.2(7)
C4−C7−C8	94.4(13)	C4−C7−C8	91.8(7)
C3−C8−C7	86.3(12)	C3−C8−C7	88.4(8)
C3−C8−C9	116.7(16)	C3−C8−C9	117.5(9)
C8−C9−C10	116.4(16)	C8−C9−C10	117.4(9)
C7−C8−C9	108.6(14)	C7−C8−C9	107.8(9)
P2−C10−C9	115.9(14)	P2−C10−C9	113.5(8)

The NMR spectroscopic data for $(DPTCT)PdCl_2$ are consistent with the structure. The ^{31}P chemical shifts[41] suggest the presence of a coordinated phospholene phosphorus atom in a six-membered chelate ring (δ 34.84) and a 7-phosphanorbornene phosphorus atom that is also part of a six-membered chelate ring (δ 97.60). The magnitude of $^2J(PP) = 28.01$ Hz is typical for *cis*-square planar palladium(II) diphosphine complexes. The ^1H NMR spectrum contains six methyl resonances, three vinyl proton resonances, and four methine resonances, two of which (H_3 and H_4) exhibit large magnitude $J(PH)$ couplings typical of methine hydrogens *anti* to phosphorus in rigid ring systems.[41] The $^{13}C\{^1H\}$ NMR spectrum contains six methyl resonances, one of which, $CH_3(16)$ displays a $^3J(PC)$ of 3.02 Hz for the same reason. There are also four aliphatic methine, two olefinic methine, and four quarternary olefinic resonances. The proton and carbon assignments were confirmed by ^{31}P decoupling, appropriate two-dimensional, and APT spectra.

(41) Nelson, J. H. In *Phosphorus-31 NMR Spectral Properties in Compound Characterization and Structural Analysis*, Quin, L. D., Verkade, J. G., Eds.; VCH: Deerfield, Beach, FL, 1994; pp. 203−214.

Table 5. Selected bond lengths (Å) and angles (deg) for [(DMPP)$_2$(*exo*-methylene)]PdBr$_2$ and [(DMB^{t}P)$_2$(*exo*-methylene)]PtBr$_2$

Bond Lengths

[(DMPP)$_2$(*exo*-methylene)]PdBr$_2$		[(DMB^{t}P)$_2$(*exo*-methylene)]PtBr$_2$	
Pd−Br1	2.489(2)	Pt−Br1	2.484(1)
Pd−Br2	2.487(2)	Pt−Br2	2.491(2)
Pd−P1	2.219(3)	Pt−P1	2.214(3)
Pd−P2	2.213(4)	Pt−P2	2.219(3)
P1−C1	1.860(12)	P1−C1	1.86(1)
P1−C4	1.779(12)	P1−C4	1.77(1)
P2−C7	1.85(12)	P2−C7	1.84(1)
P2−C10	1.801(16)	P2−C10	1.79(1)
C1−C2	1.557(8)	C1−C2	1.48(2)
C1−C7	1.555(18)	Cl−C7	1.55(2)
C2−C3	1.506(19)	C2−C3	1.49(2)
C2−C5	1.527(18)	C2−C5	1.40(2)
C3−C4	1.330(20)	C3−C4	1.36(2)
C7−C8	1.523(22)	C7−C8	1.46(2)
C8−C9	1.489(24)	C8−C9	1.43(2)
C8−C12	1.336(22)	C8−C12	1.42(2)
C9−C10	1.342(25)	C9−C10	1.29(2)

Bond Angles

[(DMPP)$_2$(*exo*-methylene)]PdBr$_2$		[(DMB^{t}P)$_2$(*exo*-methylene)]PtBr$_2$	
Br1−Pd−Br2	97.2(1)	Br1−Pt−Br2	88.90(6)
Br1−Pd−P2	90.7(1)	Br1−Pt −P2	91.42(8)
Br2−Pd−P1	87.2(1)	Br2−Pt−P1	92.58(8)
P1−Pd−P2	85.3(1)	P1−Pt−P2	86.5(1)
C1−P1−C4	92.9(6)	C1−P1−C4	93.5(7)
C7−P2−C10	94.0(6)	C7−P2−C10	92.0(6)
P1−C1−C2	104.4(8)	P1−C1−C2	107.7(9)
P1−C1−C7	109.8(8)	P1−C1−C7	113.5(6)
C2−C1−C7	118.7(11)	C2−C1−C7	114(1)
C1−C2−C3	108.8(11)	C1−C2−C3	110(1)
C1−C2−C5	112.6(10)	C1−C2−C5	123(2)
C3−C2−C5	111.7(11)	C3−C2−C5	114(1)
C2−C3−C4	117.1(11)	C2−C3−C4	118(1)
P1−C4−C3	112.1(10)	P1−C4−C3	110(1)
P2−C7−C1	111.6(8)	P2−C7−C1	113.8(7)
P2−C7−C8	103.4(9)	P2−C7−C8	105.5(8)
C1−C7−C8	113.7(11)	C1−C7−C8	114.8(9)
C7−C8−C9	112.3(13)	C7−C8−C9	113(1)
C7−C8−C12	127.7(16)	C7−C8−C12	119(2)
C9−C8−C12	120.0(18)	C9−C8−C12	120(1)
C8−C9−C10	115.2(16)	C8−C9−C10	117(1)
P2−C10−C9	111.4(11)	C2−C10−C9	112(1)

Table 6. Selected Bond Lengths (Å) and Angles (deg) for (DPTCT)PdCl$_2$

Bond Lengths

Pd−Cl1	2.369(2)	Pd−Cl2	2.381(2)
Pd−P1	2.208(7)	Pd−P2	2.218(2)
P1−C1	1.844(6)	P1−C4	1.839(7)
P2−C19	1.770(8)	P2−C22	1.824(6)
C2−C3	1.33(1)	C14−C15	1.33(1)
C19−C20	1.32(1)		

Bond Angles

Cl1−Pd−Cl2	95.48(7)	Cl1−Pd−P2	92.09(7)
Cl1−Pd−P1	175.34(7)	Cl2−Pd−P2	171.36(6)
Cl2−Pd−P1	86.49(6)	P2−Pd−P1	86.27(6)
C19−P2−C22	92.3(3)	C1−P1−C4	82.4(3)
P2−C22−C16	117.8(4)	C1−C16−C22	109.5(5)

The structure of [(DMPP)$_2$(*exo*-methylene)]PdBr$_2$ was also confirmed by multinuclear NMR spectroscopy (see Experimental Section). Of particular note is the fact that this molecule, like its platinum analogues,[2] is formd as a racemic mixture of a single diastereomer by stereospecific hydrogen transfer of H$_4$. This means that the C−C coupling to form a biradical intermediate, as previously discussed,[2] occurs in a *syn*-fashion. This results in H$_3$ and H$_4$ being *syn* in the products. Except for (DPTCT)PdCl$_2$, the other palladium chloride products illustrated

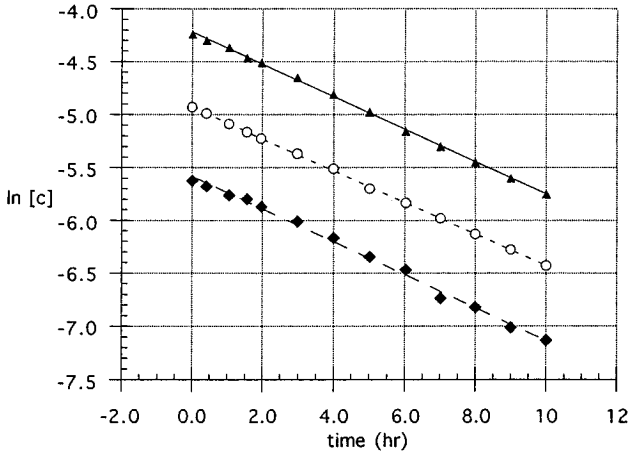

Figure 8. First-order plot for the disappearance of *cis*-(DMPP)$_2$PdCl$_2$ in Cl$_2$CHCHCl$_2$ at 145°: ♦, 0.0036 M; ○, 0.0072 M; ▲, 0.0144 M. The average apparent value of the rate constant is $(4.25 \pm 0.3) \times 10^{-5}$ s^{-1}.

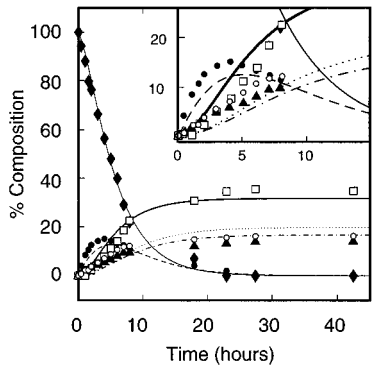

Figure 9. Percent composition as a function of time for the thermolysis of *cis*-(DMPP)$_2$PdCl$_2$ in Cl$_2$CHCHCl$_2$ at 145 °C: ♦, starting material; ●, [4 + 2]; ○, *exo*-methylene; ▲, [2 + 2]; □, (DPTCT)PdCl$_2$. The lines were calculated from the following rate constants: $k_1 = (1.5 \pm 0.3) \times 10^{-5}$ s^{-1}; $k_2 = (2.9 \pm 0.3) \times 10^{-5}$ s^{-1}; $k_3 = (3.4 \pm 0.3) \times 10^{-5}$ s^{-1}; $k_4 = (2.5 \pm 0.3) \times 10^{-5}$ s^{-1}; $k_5 = (1.0 \pm 0.3) \times 10^{-4}$ M^{-1} s^{-1}.

Table 7. ^{31}P{^{1}H} NMR Data at 121.65 MHz for the Products of Thermolysis of (DMPP)$_2$PdX$_2$ Complexes in CDCl$_3$ at 300 K (δ, ppm; J Hz)

	δ^{31}P	^2J(PP)
	X = Cl	
[4 + 2]	133.67, 58.58	12.29
[2 + 2]	107.42	
[*exo*-methylene]	107.26, 93.26	10.22
[DPTCT]	97.60, 34.84	28.10
	X = Br	
[4 + 2]	134.16, 58.10	11.50
[2 + 2]	108.76	
[*exo*-methylene]	108.47, 94.62	16.97
[DPTCT]	94.65, 31.52	23.42

in Scheme 1 were not isolated but were only characterized by ^{31}P{^{1}H} NMR spectroscopy of the reaction mixtures. Assignments (Table 7) were made by comparison with the data for the analogous platinum complexes.[2]

Kinetics. Detailed kinetics of the solid-state thermolyses were not obtained. The same products in the same final ratios were formed in both the solid- and solution-state thermolyses, suggesting that the mechanisms are the same.

Detailed kinetic runs were performed on reactions of *cis*-(DMPP)$_2$PdCl$_2$ in 1,1,2,2-tetrachloroethane at 145 °C. The results are shown in Figures 8 and 9. The overall loss of starting material is clearly first order (Figure 8), implying a unimolecular mechanism. A proposed mechanism is shown in Scheme 2. Though the [2 + 2], [4 + 2], and *exo*-methylene products could

Scheme 2

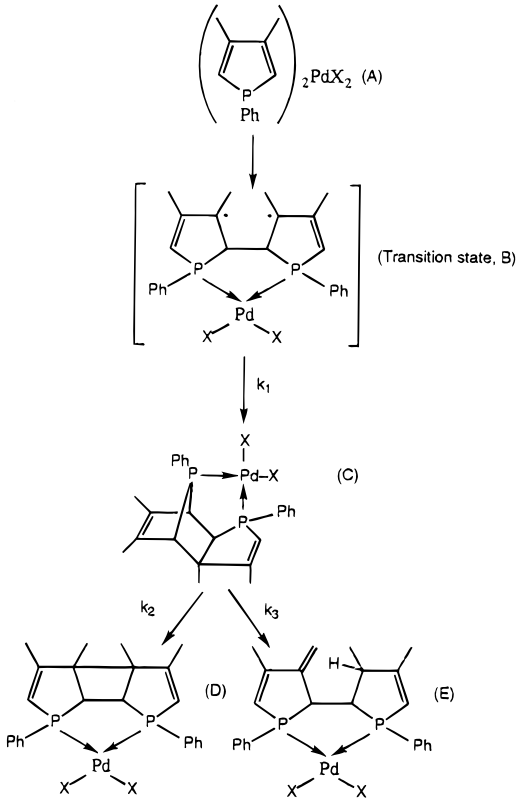

also be formed by independent electrocyclic and ene reactions, we favor the mechanism shown in Scheme 2 for its simplicity.

The starting material (A) may react by forming a bond between carbons 1 and 1′ of two adjacent phospholes to generate a diallyl 1,4-biradical transition state (B). This transition state could collapse by additional carbon−carbon bond formation to the observed [4 + 2] species (C). As can be seen from Figure 9, the [4 + 2] product is subsequently converted to the [2 + 2] (D) and *exo*-methylene (E) products. We assume, in contrast to what was found[2] for the thermolyses of *cis*-$(DMPP)_2PtCl_2$, that both the [2 + 2] and *exo*-methylene products are formed irreversibly. Thus, the unimolecular reaction is ultimately driven to the [2 + 2] and *exo*-methylene products.

In addition to this unimolecular reaction pathway there is also a parallel bimolecular reaction pathway for the formation of $(DPTCT)PdCl_2$, a proposed mechanism for which is shown in Scheme 3.

These two pathways give rise to the following rate laws, eqs 3−8.

$$-\mathrm{d[A]}/\mathrm{d}t = (k_1 + k_4)[\mathrm{A}] + k_5[\mathrm{A}][\mathrm{F}] \quad (3)$$

$$\mathrm{d[C]}/\mathrm{d}t = k_1[\mathrm{A}] - (k_2 + k_3)[\mathrm{C}] \quad (4)$$

$$\mathrm{d[D]}/\mathrm{d}t = k_2[\mathrm{C}] \quad (5)$$

$$\mathrm{d[E]}/\mathrm{d}t = k_3[\mathrm{C}] \quad (6)$$

$$\mathrm{d[F]}/\mathrm{d}t = k_4[\mathrm{A}] - k_5[\mathrm{A}][\mathrm{F}] \quad (7)$$

$$\mathrm{d[G]}/\mathrm{d}t = \mathrm{d[X]}/\mathrm{d}t = k_5[\mathrm{A}][\mathrm{F}] \quad (8)$$

According to this mechanism, the loss of starting material should be first order in starting material and an approximate value of $(k_1 + k_4) = (4.25 \pm 0.3) \times 10^{-5}$ s^{-1} is directly determined. Approximate values of k_2 and k_3 were determined from the initial rates of formation of D and E, respectively. Then

Scheme 3

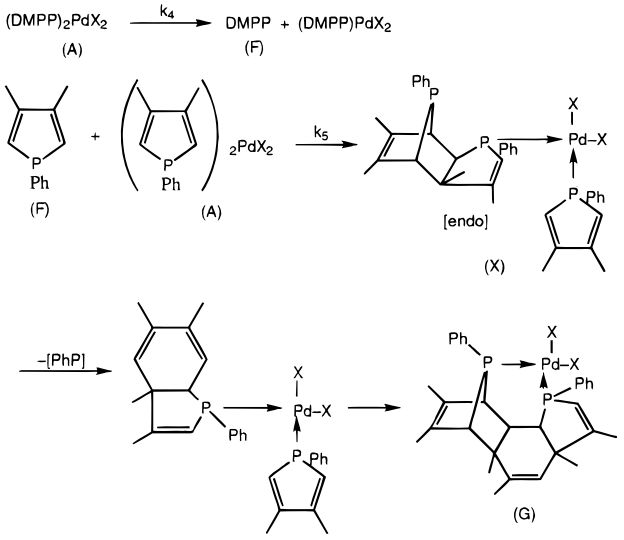

eqs 3−8 were integrated numerically to find the temporal behavior of the concentration of each species. The calculated percent composition of the reaction mixture was based on the relative amounts of A, C, D, E, G, and unidentified products, with the amounts of G and unidentified products being assumed to be equal to each other. The rate constants were then adjusted to give the fit to the experimental data.

The validity of this mechanism is shown in the concentration *vs* time graph of the various components (Figure 9). Since the rate of formation of the [4 + 2] cycloaddition product is approximately one-fourth its rate of conversion to the [2 + 2] and *exo*-methylene products, its concentration peaks early in the reaction and ultimately decreases to zero. Note also that the initial rate of formation of the *exo*-methylene product is only 1.2 times that of the [2 + 2] product and this is the approximate final ratio of these two products.

An attempt was made to model the kinetics of the thermolysis of *cis*-$(DMPP)_2PdCl_2$ by the same rate laws that were found[2] for the thermolysis of *cis*-$(DMPP)_2PtCl_2$ but without success. Also, in contrast to what was observed for the thermolysis of the platinum complex where the solid-state ($k_1 = (6.1 \pm 0.3) \times 10^{-5}$ s^{-1}) reaction was slightly slower than the reaction in solution ($k_1 = (8.33 \pm 0.3) \times 10^{-5}$ s^{-1}), for the palladium complex the reaction in the solid state is much faster than that in solution. This is probably related to the fact that for the reactions of the palladium complexes there are two parallel reaction pathways, whereas for the reactions of the platinum complexes there is only one pathway. The complex concentration is maximized in the solid state such that the reaction in the solid state might be expected to be faster than that in solution.

The thermolysis of *trans*-$(DMPP)_2PdBr_2$ is faster in solution than in the solid state. This is probably because isomerization to the *cis*-isomer must first occur before the intramolecular phosphole coupling reactions may proceed. The two isomers are in rapid dynamic equilibrium in solution, but the solid-state isomerization is slow.

The exact reasons why the palladium reactions contain two pathways and the platinum reactions do not are unknown. If one compares the crystal packing diagrams for *cis*-$(DMPP)_2PdCl_2$[17] and *cis*-$(DMPP)_2PtCl_2$,[42] we see that in fact two complex molecules are somewhat closer in space for the palladium complex, where the distance between the centroids of two phosphole rings on adjacent complexes is 7.08 Å, than

(42) Holt, M. S.; Nelson, J. H.; Alcock, N. W. *Inorg. Chem.* **1986**, *25*, 2288.

for the platinum complex where the corresponding distance is 8.26 Å. *trans*-$(DMPP)_2PdBr_2$ undergoes thermal isomerization to *cis*-$(DMPP)_2PdBr_2$ in the solid state, most likely by dissociation and reassociation of a phosphole. This observation is consistent with the bimolecular mechanism for the formation of $(DPTCT)PdX_2$ shown in Scheme 3. If the rate determining step in this process is the dissociation of phosphole, then the disappearance of $(DMPP)_2PdX_2$ would be first order and the unimolecular and ultimately bimolecular reactions would be parallel processes. The fate of $(DMPP)PdX_2$ and the phosphinidene, PhP, are unknown. There are, however, unidentified phosphorus containing products formed together with some elemental palladium. No elemental platinum was observed in the thermolyses of the platinum complexes.

Conclusions

The thermolyses of $(DMPP)_2PdX_2$ complexes proceed *via* parallel bimolecular ($k_5 = (1.0 \pm 0.3) \times 10^{-4}$ M^{-1} s^{-1}) and branched unimolecular ($k_1 = (1.5 \pm 0.3) \times 10^{-5}$ s^{-1}) processes. The branches in the unimolecular process may evolve from a common 1,4-butanediyl biradical[43] transition state. In both the solution and solid states the reaction proceeds only from the *cis*-$(DMPP)_2PdX_2$ complexes. For $(DMPP)_2PdBr_2$ this results from *trans* ⇌ *cis* isomerization equilibria extant in both the solution and solid states. The *trans*-geometry precludes intramolecular carbon−carbon bond formation. The nature of the halide affects the reaction only in the determination of the geometry of the complexes. The larger the halide, the more thermodynamically stable the *trans* isomer. There are minimal differences in the reaction rates and product distributions between the chloride and bromide complexes in solution. In the solid state there are notable differences in the rates but not the final product distributions. No reaction occurs for the iodide complex, which has the *trans* geometry in both states. The palladium complexes slowly dissociate phosphole to some extent, and this leads to bimolecular products. The platinum complexes do not dissociate phosphole, and for them no bimolecular products are observed. The reaction rates are not influenced by added halide in the form of $[Me_4N]^+X^-$ (X = Cl, Br), but phosphole inhibition studies could not be undertaken because the presence of excess phosphole in solution leads to rapid ligand exchange through formation of pentacoordinate $(DMPP)_3MX_2$ complexes.[44]

Acknowledgment. We are grateful to the donors of the Petroleum Research Fund, administered by the American Chemical Society, for financial support, to the National Science Foundation (Grant CHE-9214294) for funds to purchase the 500 MHz NMR spectrometer, and to Professor Derek J. Hodgson and Dr. Urszula Rychlewska of the University of Wyoming for assistance with the crystal packing diagrams.

Supporting Information Available: For the crystal structures, tables listing crystal and refinement data, bond distances and angles, H atom coordinates, and thermal parameters (23 pages). Ordering information is given on any current masthead page.

IC951307F

(43) For recent discussions of biradical intermediates, see: Peterson, T. H.; Carpenter, B. K. *J. Am. Chem. Soc.* **1992**, *114*, 1496. Ariel, S.; Evans, S. V.; Garcia-Garisbay, M.; Harkness, B. R.; Omkaram, N.; Scheffer, J. R.; Trotter, J. *J. Am. Chem. Soc.* **1988**, *110*, 5591.

(44) MacDougall, J. J.; Nelson, J. H.; Mathey, F. *Inorg. Chem.* **1982**, *21*, 2145.